SEMARAK ILMU PUBLISHING

Journal of Advanced Research in Fluid Mechanics and Thermal Sciences

Journal homepage:
https://semarakilmu.com.my/journals/index.php/fluid_mechanics_thermal_sciences/index
ISSN: 2289-7879

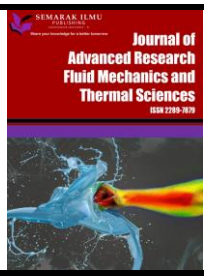

Mathematical Model of Reiner-Philippoff Embedded with Al_2O_3 and Cu Particles over a Shrinking Sheet with Mixed Convection and Mass Flux Effect

Nur Syahidah Nordin[1,3], Hussein Ali Mohammed Al-Sharifi[2], Abdul Rahman Mohd Kasim[1,5,*], Iskandar Waini[4], Masyfu'ah Mokhtar[1,3], Mohd Fakhizan Romlie[6], Dafrizal Samsudin[7], Didit Adytia[8]

[1] Centre for Mathematical Sciences, Universiti Malaysia Pahang Al-Sultan Abdullah, Gambang, 26300 Kuantan, Pahang, Malaysia
[2] Department of Mathematics, College of Education for Pure Sciences, University of Kerbala, 1125, Karbala, Iraq
[3] Mathematical Sciences Studies, College of Computing, Informatics and Media, Universiti Teknologi MARA (UiTM) Johor Branch, Segamat Campus, 85000 Segamat, Johor, Malaysia
[4] Fakulti Teknologi Kejuruteraan Mekanikal dan Pembuatan, Universiti Teknikal Malaysia Melaka, Hang Tuah Jaya, Durian Tunggal 76100, Melaka, Malaysia
[5] Center for Research in Advanced Fluid and Process, University Malaysia Pahang, Lebuhraya Tun Razak, Gambang, Kuantan, 26300, Pahang, Malaysia
[6] Department of Electrical and Electronic Engineering, Universiti Teknologi PETRONAS, 32610, Seri Iskandar, Perak, Malaysia
[7] Program Studi Ilmu Komunikasi, Fakultas Ilmu Komunikasi, Universitas Islam Riau, Jalan Kaharuddin Nst No.113, Simpang Tiga, Kec. Bukit Raya, Kota Pekanbaru, Riau, Indonesia
[8] School of Computing, Telkom University, Jalan Telekomunikasi No. 1 Terusan Buah Batu, Bandung 40257, Indonesia

ARTICLE INFO

Article history:
Received 15 August 2023
Received in revised form 3 November 2023
Accepted 14 November 2023
Available online 30 November 2023

Keywords:
Mixed convection; hybrid nanofluid; Reiner-Philippoff; mass flux; shrinking sheet

ABSTRACT

The investigation on the Reiner–Philippoff fluid model embedded with two different nanoparticles (Al_2O_3 and Cu) over a shrinking sheet is carried out. The Tiwari and Das model are applied in the study covering the continuity, momentum, energy equations, and Reiner-Philippoff relation. The flow studied also considers the mixed convection and mass flux influences. The respective equations are first transformed into ordinary differential equation form using the similarity transformation before performing the computation work using the bvp4c function in MATLAB. The present model is identical to the established model in special cases, and then a direct comparative study is executed to verify the current model. The results for respective problems are presented in tabular and graphical form. It is perceived that the presence of nanoparticles affects the fluid characteristic significantly.

1. Introduction

An efficient working fluid is required for industrial and technological applications to regulate processes and produce superior final products. Although many processes use non-Newtonian fluid types to accelerate advancements, pure water (Newtonian) is still used as a cooling agent. There are various non-Newtonian fluids, and each has distinctive properties. In contrast to Newtonian fluid,

* *Corresponding author.*
E-mail address: rahmanmohd@umpsa.edu.my

https://doi.org/10.37934/arfmts.111.2.195213

whose strain is by the stress tensor, the non-Newtonian fluid type is classified by either shear thinning, which displays pseudo-plasticity, or shear thickening, which describes the dilatant. Shear-thinning fluids show the behaviour of Newtonian fluids at extreme shear rates, whereas shear-thickening fluids show the development in viscosity proportional to shear rate. Krishnan *et al.,* [1] indicates that the fluid in models reflecting shear thickening and shear thinning characteristics includes the Powell-Eyring, Sisko, Carreau-Yasuda, and Carreau viscosity models and Reiner-Philippoff.

The Reiner-Philippoff model, which belongs to the non-Newtonian group, is the most fascinating to study because it exhibits Newtonian fluid behaviour at low or high values (shear stress) and non-Newtonian behaviour at other values. Furthermore, the Reiner-Philippoff model is essential and unique in representing natural fluid in industrial applications. In certain situations, it can exhibit three fluid characteristics where it can behave like Newtonian, dilatant, and pseudo-plastics. This is significant in manufacturing procedures since the applied fluid might vary in a specific process to achieve the best production. In addition, numerous researches examined the flow's movement over various geometries and its effects on the flow field [2-11].

The study of fluid flow has advanced and become more fascinating since the development of nanofluids, which can control heat and mass transfer and flow behaviour. In the industrial engineering and manufacturing processes, the boundary layer flow triggered by the stretching or shrinking surface is widely employed, such as in wire drawing, continuous glass casting, and polymer or metal extrusions. The flow across a linearly stretched surface appears to have been studied for the first time historically by Crane [12]. Flows over shrinking surfaces have recently drawn attention, in contrast to flows over stretched surfaces. The flow that the shrinking surface causes is effectively a reverse flow, claims Goldstein [13]. In addition, numerous researches have examined the impact of various physical parameters on stretching and shrinking surfaces [14-23].

Convection heat transfer is a process caused by differences in temperature and density, through which heat is transferred from one part of the fluid to another. There are two types of convection: forced convection and natural convection. Forced convection is the process of fluid motion imparted by an external source, while natural convection is caused by natural means such as buoyancy effects. Mixed convection is formed when forced and natural convection systems combine. Due to its significance in industrial systems, including nuclear reactors, solar collectors, and electronic devices, mixed convection flow is a topic of great interest to researchers. Merkin [24] examined the mixed convection flow toward a vertical plate in a porous material. Ingham [25] researched the mixed convection flow over a moving vertical flat plate. Ramachandran *et al.,* [26] then applied this work to the stagnation flow problem and discovered that the opposing flow area was where the solution's non-uniqueness occurred. In addition, previous researches have also considered the work on the mixed convection flow over various geometry [27-31].

In recent years, hybrid nanofluids have replaced nanofluids in several technologies to enhance thermal performance. Turcu *et al.,* [32] and Jana *et al.,* [33] are among the first researchers to integrate hybrid nano-composite particles in their experimental work. Due to the synergistic effects of its various nanoparticles, a hybrid nanofluid is an innovative fluid that can accelerate the heat transfer rate [34]. The appropriate nanoparticles can also be combined or hybridized to achieve the optimum heat transfer [35]. Suresh *et al.,* [36] created a nanocrystalline Cu- Al_2O_3 hybrid nanocomposite using a thermochemical process. Then, the produced nanocomposite powder was dissolved in deionized water to form the hybrid Cu-Al_2O_3/water nanofluid. The experimental findings show that nanoparticles' volume concentration increases with the hybrid nanofluid's thermal conductivity and viscosity. When the viscosity and thermal conductivity of the nanofluids were examined, it was found that the viscosity increase was considerably more than the thermal

conductivity increase. Moreover, they claimed that even while alumina has a low heat conductivity, it has a good level of chemical inertness, which could help to keep the hybrid nanofluid stable. Suresh *et al.,* [37] investigated the pressure drop characteristics of the Cu-Al_2O_3/water hybrid nanofluid and laminar convection heat transfer in uniformly heated circular tubes. Compared to the Nusselt number of waters, the testing results show a maximum rise in the Nusselt number of 13.56%. 0.1% hybrid Cu- Al_2O_3/water nanofluid has a slightly higher friction factor than 0.1% Al_2O_3/water nanofluid. Because of Suresh's discoveries, Cu- Al_2O_3/water is an incredibly efficient hybrid nanofluid in transferring heat. Additionally, Singh and Sarkar [38] and Farhana *et al.,* [39] also commented on the relevance of the combination of alumina and other nanoparticles. In this regard, Devi and Devi [40] investigated the Al_2O_3-Cu hybrid nanofluid boundary layer flow problem across a stretching surface using new correlations of the thermophysical properties that matched the findings of Suresh *et al.,* [37]. They found that the higher nanoparticle volume fractions enhanced the heat transfer rate in those studies. In recent years, a hybrid nanofluid's boundary layer flow past a stretching or shrinking surface has been thoroughly studied. The significance of this field's uses in manufacturing processes, such as synthetic fiber synthesis, paper manufacture, and polymer extraction, has led to a tremendous rise in studies in this area. Waini *et al.,* [41] reported a temporal stability analysis on the flow via a stretching and shrinking surface in a hybrid nanofluid. They found that one of the solutions was unstable over time, whilst the other was stable and physically trustworthy.

Motivated by the above literature survey, this study focuses on the mixed convection of Reiner-Philippoff hybrid nanofluid. The flow is expected to pass across a shrinking sheet. Also, as water is regarded as a base fluid, Al_2O_3-Cu nanohybrid particles are added to the based fluid to expedite the heat transfer rate. Influences from mass flux are also considered in the flow. The governing equations are derived into ordinary differential equation form using the similarity transformation before it is solved computationally using the bvp4c function in MATLAB. The findings are presented graphically and briefly discuss how various physical factors were influenced. This problem has not been studied before, so the reported results are new.

2. Methodology

Figure 1 depicts the physical configuration of Reiner-Philippoff nanofluid across a shrinking surface where the velocity's surface is $u = ax^{1/3} f'(\eta)$ with $a > 0$. The mass flux velocity $v_w(x)$ represents the surface permeability, while given $T_w = T_\infty + T_0 x^{-1/3}$ is the surface temperature where the constant ambient temperature is T_∞ and T_0 is the reference temperature. Thus, the comprehensive equations for the suggested model are as follows [10,31]:

$$\frac{\partial u}{\partial x} + \frac{\partial v}{\partial y} = 0 \tag{1}$$

$$\frac{\partial u}{\partial y} = \frac{\tau}{\mu_\infty + \dfrac{\mu_{hnf} - \mu_\infty}{1 + \left(\dfrac{\tau}{\tau_s}\right)^2}} \tag{2}$$

$$u\frac{\partial u}{\partial x} + v\frac{\partial u}{\partial y} = \frac{1}{\rho_{hnf}}\frac{\partial \tau}{\partial y} + \frac{(\rho\beta_T)_{hnf}}{\rho_{hnf}} g\left(T - T_\infty\right) \tag{3}$$

$$u\frac{\partial T}{\partial x}+v\frac{\partial T}{\partial y}=\frac{k_{hnf}}{\left(\rho C_p\right)_{hnf}}\frac{\partial^2 T}{\partial^2 y} \tag{4}$$

subject to:

$$\begin{aligned} &u=\varepsilon u_w(x),\ v=v_w(x),\ T=T_w \ \text{ at } \ y=0\\ &u\to 0,\ \ T\to T_\infty \ \text{ as } \ y\to\infty \end{aligned} \tag{5}$$

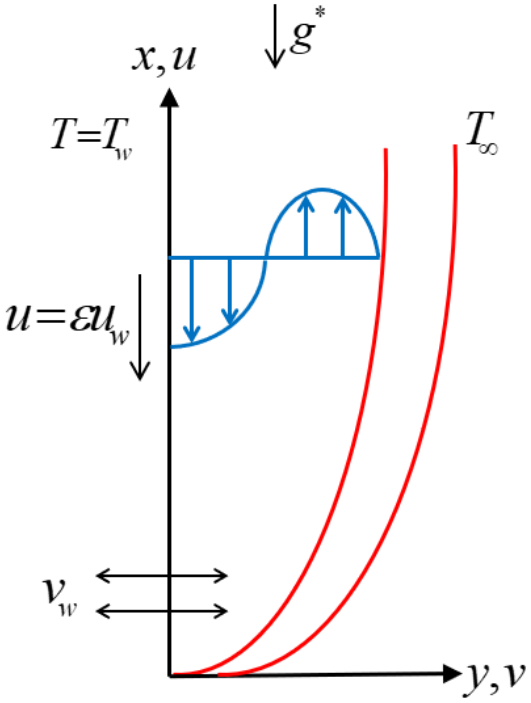

Fig. 1. The physical model

where (u,v) are the velocity components in the (x,y) directions, respectively. Further, ρ_{hnf} is fluid density, $(\rho\beta)_{hnf}$ is thermal expansion, $\left(\rho C_p\right)_{hnf}$ is heat capacity, k_{hnf} is thermal conductivity, μ_{hnf} is dynamic viscosity, μ_∞ is limiting dynamic viscosity, *T* is temperature, *g* is acceleration due to gravity, τ is shear stress of Reiner-Philippoff fluid, τ_s is references shear stress and ε is stretching/shrinking parameter. The subscripts of *hnf* and *f* stand for hybrid nanofluid and fluid, respectively. The similarity transformation is as follows [42]:

$$\psi=\sqrt{a\nu x^{1/3}}\,f(\eta),\qquad \tau=\rho\sqrt{a^3\nu}\,g(\eta),\qquad \theta(\eta)=\frac{T-T_\infty}{T_w-T_\infty},\qquad \eta=\frac{y}{x^{1/3}}\sqrt{\frac{a}{\nu}} \tag{6}$$

The term ψ is express by $u=\partial\psi/\partial y$ and $v=-\partial\psi/\partial x$ yield:

$$u=ax^{1/3}f'(\eta),\qquad v=-\sqrt{a\nu_f}\,x^{-1/3}\left(\frac{2}{3}f(\eta)-\frac{1}{3}\eta f'(\eta)\right) \tag{7}$$

At $\eta = 0$, the wall mass flux velocity obtained as:

$$v_w(x) = -\frac{2}{3}\sqrt{a\nu_{hnf}}\,x^{-1/3}S \tag{8}$$

in which $f(0) = S$ indicates the parameter of constant mass flux. There are three different situations of the value of *S*, where *S* = 0 denote the impermeable surface, *S* < 0 for injection and *S* > 0 is for suction, while $\nu_f = \mu_\infty/\rho_f$ is the fluid kinematic viscosity. The similarity between Eq. (9) to Eq. (12) are obtained after employing Eq. (6) and Eq. (7):

$$g = f''\left(\frac{g^2 + \left(\frac{\mu_{hnf}}{\mu_f}\right)\lambda\gamma^2}{g^2+\gamma^2}\right) \tag{9}$$

$$g' - \frac{\rho_{hnf}}{\rho_f}\left(\frac{1}{3}f'^2 - \frac{2}{3}ff''\right) + \left[\frac{(\rho\beta_T)_{hnf}}{(\rho\beta_T)_f}\right]Z\theta = 0 \tag{10}$$

$$\frac{1}{\mathrm{Pr}}\left[\frac{k_{hnf}}{k_f}\right]\theta'' + \left[\frac{(\rho C_p)_{hnf}}{(\rho C_p)_f}\right]\left(\frac{1}{3}f'\theta + \frac{2}{3}f\theta'\right) = 0 \tag{11}$$

subject to:

$$\begin{aligned} &f(0) = S,\ f'(0) = \varepsilon,\ \theta(0) = 1 \\ &f'(\eta) \to 0,\ \ \theta(\eta) \to 0 \ \text{ as } \ \eta \to \infty \end{aligned} \tag{12}$$

The dimensionless parameter Bingham number *γ*, Reiner–Philippoff fluid *λ*, mixed convection *Z*, and Prandtl number Pr, are defined by:

$$\gamma = \frac{\tau_s}{\rho_f\sqrt{a^3\nu_f}}, \qquad \lambda = \frac{\mu_f}{\mu_\infty}, \qquad Z = \frac{Gr}{\mathrm{Re}_x^2} = \frac{g(\beta_T)_f T_0}{a^2}, \qquad \mathrm{Pr} = \frac{(\mu C_p)_f}{k_f} \tag{13}$$

Note that *λ* = 1 presents viscous Newtonian type, whereas *λ* > 1 signifies the shear-thinning and *λ* < 1 is the shear-thickening fluid type, respectively. Further, *ε* = 0 signifies the static sheet, *ε* > 0 indicates the stretching sheet, and *ε* < 0 is the shrinking sheet. The quantity of physical in terms of skin friction and local Nusselt number is given by:

$$C_f = \frac{\tau_w}{\rho_f u_w^2}, \quad Nu_x = \frac{xq_w}{k_f(T_w - T_\infty)} \tag{14}$$

where

$$\tau_w = \rho_f \sqrt{a^3 \nu_f}\left(g(\eta)\right)_{y=0}, \qquad q_w = -k_{hnf}\left(\frac{\partial T}{\partial y}\right)\Big|_{y=0} \tag{15}$$

The τ_w symbolizes the quantity of τ on $y = 0$, and q_w presenting the surface heat flux. Then, one gets:

$$\mathrm{Re}_x^{1/2} C_f = g(0), \qquad \mathrm{Re}_x^{-1/2} Nu_x = -\frac{k_{hnf}}{k_f}\theta'(0) \tag{16}$$

where $Re_x = u_w(x)x/v_f$ is the local Reynolds number and $Gr_x = \left(g^*(\beta_T)_f\left(T_0 x^{-1/3}\right)x^3\right)/v_f^2$ is the Grashof number. The physical properties of water, Al_2O_3, and Cu are listed in Table 1, whereas the thermophysical characteristics of nanofluid and hybrid nanofluid are listed in Table 2. Meanwhile, the nanoparticle volume fractions of Al_2O_3 and Cu are symbolized by ϕ_1 and ϕ_2, respectively. Also, the subscripts of *hnf, nf,* and *f*, stand for hybrid nanofluid, nanofluid, and fluid, respectively.

Table 1
Thermophysical properties of water, Al_2O_3, and Cu [43]

Thermophysical properties	Water	Al_2O_3	Cu
$\rho\left(kg/m^3\right)$	997.1	3970	8933
$C_p\left(J/kgK\right)$	4179	765	385
$k\left(W/mK\right)$	0.613	40	400
$\beta\times10^{-5}\left(1/K\right)$	0.85	1.67	21

Table 2
Thermophysical properties of *nf* and *hnf* [44]

Thermophysical properties	Nanofluid	Hybrid nanofluid
Density	$\rho_{nf} = (1-\phi)\rho_f + \phi\rho_s$	$\rho_{hnf} = \left(1-\phi_{hnf}\right)\rho_f + \phi_1\rho_{s1} + \phi_2\rho_{s2}$
Heat capacity	$\left(\rho C_p\right)_{nf} = (1-\phi)\left(\rho C_p\right)_f + \phi\left(\rho C_p\right)_s$	$\left(\rho C_p\right)_{hnf} = (1-\phi)_{hnf}\left(\rho C_p\right)_f + \phi_1\left(\rho C_p\right)_{s1} + \phi_2\left(\rho C_p\right)_{s2}$
Dynamic viscosity	$\frac{\mu_{nf}}{\mu_f} = \frac{1}{(1-\phi)^{2.5}}$	$\frac{\mu_{hnf}}{\mu_f} = \frac{1}{\left(1-\phi_1-\phi_2\right)^{2.5}}$
Thermal conductivity	$\frac{k_{nf}}{k_f} = \frac{k_s + 2k_f - 2\phi\left(k_f - k_s\right)}{k_s + 2k_f + 2\phi\left(k_f - k_s\right)}$	$\frac{k_{hnf}}{k_f} = \frac{\frac{\phi_1 k_1 + \phi_2 k_2}{\phi_{hnf}} + 2k_f + 2\left(\phi_1 k_1 + \phi_2 k_2\right) - 2\phi_{hnf} k_f}{\frac{\phi_1 k_1 + \phi_2 k_2}{\phi_{hnf}} + 2k_f - 2\left(\phi_1 k_1 + \phi_2 k_2\right) - 2\phi_{hnf} k_f}$
Thermal expansion coefficient	$(\rho\beta)_{nf} = (1-\phi)(\rho\beta)_f + \phi(\rho\beta)_s$	$(\rho\beta)_{hnf} = \left(1-\phi_{hnf}\right)(\rho\beta)_f + \phi_1(\rho\beta)_{s1} + \phi_2(\rho\beta)_{s2}$ where $\phi_{hnf} = \phi_1 + \phi_2$

3. Results and Discussion

The numerical solutions of Eq. (9) to Eq. (12) are obtained using the boundary value problem solver, bvp4c, a feature of the MATLAB software. It uses the three-stage Lobatta IIIa formula and is a finite difference approach. To acquire the necessary solutions, the selection of initial guess and boundary layer thickness η_∞ will depend on the parameters used. This solver is also being utilized by various researchers to solve boundary layer flow problems [45-49].

A direct comparison analysis is conducted on the existing value of $f''(0)$ provided by Cortell [50], Ferdows *et al.,* [51], and Waini *et al.,* [18] to vouch for the dependability of the current model. It should be noted that the equations on the current model were the same for the limiting case, making a comparison between the present findings and the current output appropriate. In Table 3 and Table 4, respectively, the validation data on the values of $f''(0)$ are presented. The comparison reveals excellent agreement, which supports the current mathematical formulation and the provided numerical results.

Table 3
Comparative model in terms of momentum equations

Author	Model (momentum)	Limiting cases
Current	$g' - \frac{\rho_{hnf}}{\rho_f}\left(\frac{1}{3}f'^2 - \frac{2}{3}ff''\right) + \left[\frac{(\rho\beta_T)_{hnf}}{(\rho\beta_T)_f}\right] Z\theta = 0$	*Z = 0*
Cortell [50]	$3f''' + 2ff'' - (f')^2 = 0$	-
Ferdows *et al.,* [51]	$f''' + \frac{2}{3}ff'' - \frac{1}{3}\left(f'^2 + Mf'^2\right) + Gr\theta + Gc\phi = 0$	*M = Gr = Gc = 0*
Waini *et al.,* [18]	$3\frac{\mu_{hnf}/\mu_f}{\rho_{hnf}/\rho_f} f''' + 2ff'' - f'^2 = 0$	-

Table 4
Comparative value of $f''(0)$ at $\varepsilon = \lambda = \gamma = 1$, Pr = 2 and *Z* = 0 for different value of *S*

S	Cortell [50]	Ferdows *et al.,* [51]	Waini *et al.,* [18]	Current
-0.75	-0.453521	-0.453523	-0.453523	-0.453523325
-0.5	-0.518869	-0.518869	-0.518869	-0.518869429
0	-0.677647	-0.677648	-0.677648	-0.677647983
0.5	-0.873627	-0.873643	-0.873643	-0.873642863
0.75	-0.984417	-0.984439	-0.984439	-0.984439388

To strengthen the current formulation and the current output, the values of $g(0)$ are also compared with the result obtained by Sajid *et al.,* [10] and Waini *et al.,* [52] for various values of the Reiner-Philippoff fluid parameter λ, the Bingham number γ and Pr = 2. A strong agreement can be seen in the comparison; hence, Table 5 and Table 6 show the corresponding numerical values. For higher values of γ, the values of $g(0)$ significantly increase. However, with the rise of λ, there is a slight decrease in the values of $\mathrm{Re}_x^{1/2} C_f$.

Table 5

Comparative model in terms of momentum equations

Author	Model (momentum)	Limiting cases
Current	$g' - \frac{\rho_{hnf}}{\rho_f}\left(\frac{1}{3}f'^2 - \frac{2}{3}ff''\right) + \left[\frac{(\rho\beta_T)_{hnf}}{(\rho\beta_T)_f}\right]Z\theta = 0$	*Z = 0*
Sajid *et al.,* [10]	$g' + \frac{2}{3}ff'' - \frac{1}{3}f'^2 = 0$	-
Waini *et al.,* [52]	$g' + \frac{2}{3}ff'' - \frac{1}{3}f'^2 - M\sin^2(\beta)f' = 0$	*M = 0*

Table 6
Comparative value of $g(0)$ for λ and γ when $S = Z = 0$ and $\varepsilon = 1$

γ	λ	Sajid *et al.,* [10]	Waini *et al.,* [52]	Current
0.1	0.1	-0.660273	-0.660275	-0.660275189
0.5		-0.380604	-0.380604	-0.380603983
1		-0.246415	-0.246415	-0.246414994
0.1	0.3	-0.664497	-0.664498	-0.664497827
	0.5	-0.668484	-0.668486	-0.668486422
	0.7	-0.672282	-0.672277	-0.672276682

The analysis conducted for this study is shown graphically in terms of physical quantities and profile data. The values of $\mathrm{Re}_x^{1/2} C_f$ and $\mathrm{Re}_x^{-1/2} Nu_x$ for various values of dimensionless physical parameters are shown in Table 7. At a fixed value for the measured parameters (ε = -1, S = 2.4, λ = 1.5, γ = 0.1, Pr = 10 and Z = -0.5) where $\phi_1 = \phi_2 = 0$ (pure fluid), it appears that the values of $\mathrm{Re}_x^{1/2} C_f$ increase when S, Z, and Pr rise, whereas they decrease when ε, λ and γ are added. The values of $\mathrm{Re}_x^{-1/2} Nu_x$ (thermal rate) increase when ε, S, Z, and Pr are increased while it trends downward with the accession of λ and γ. Stretching flow, suction, mixed convection parameters, and a high Prandtl number are dominant phenomena that tend to release energy to the flow. On the other hand, the flow energy is slowed by the presence of the Bingham number and the Reiner-Philippoff fluid parameter. The fluctuation of $\mathrm{Re}_x^{1/2} C_f$ and $\mathrm{Re}_x^{-1/2} Nu_x$ under the influence of S and λ at constant values of ε = -1, γ = 0.1, Pr = 10 and Z = -0.5 is depicted in Figure 2 and Figure 3. The values of $\mathrm{Re}_x^{1/2} C_f$ and $\mathrm{Re}_x^{-1/2} Nu_x$ are decreased due to the rise of λ in a shrinking sheet. Larger values of λ, from a physical perspective, establish barriers to the shear-thinning effect, which lessens the fluid's interaction with surfaces and produces less drag. Meanwhile, the increase in S substantially raised the values of $\mathrm{Re}_x^{1/2} C_f$ and $\mathrm{Re}_x^{-1/2} Nu_x$.

Table 7

Values of $\mathrm{Re}_x^{1/2} C_f$ and $\mathrm{Re}_x^{-1/2} Nu_x$ for various values of physical parameters

ε	S	λ	γ	Z	Pr	$\mathrm{Re}_x^{1/2} C_f$	$\mathrm{Re}_x^{-1/2} Nu_x$
-1	2.4	1.5	0.1	-0.5	10	1.071559759	15.797838638
-0.5						0.673644536	15.902427543
1						-2.671121502	16.173117605
-1	2.35					0.983959247	15.458950581
	2.38					1.040255984	15.662372870
	2.42					1.100157249	15.933222541
	2.4	0.5				1.123427917	15.798679715
		1.2				1.089582739	15.798125718
		1.8				1.051917467	15.797528114
		1.5	0.09			1.076613256	15.797920603
			0.11			1.066023793	15.797748671
			0.15			1.037822480	15.797291518
			0.1	-0.7		1.057149539	15.797731777
				0		1.107545857	15.798105180
				0.8		1.165010666	15.798529902
				-0.5	3	0.698234629	4.597082725
					5	0.728543011	7.795010391
					12	0.765218974	18.993257535

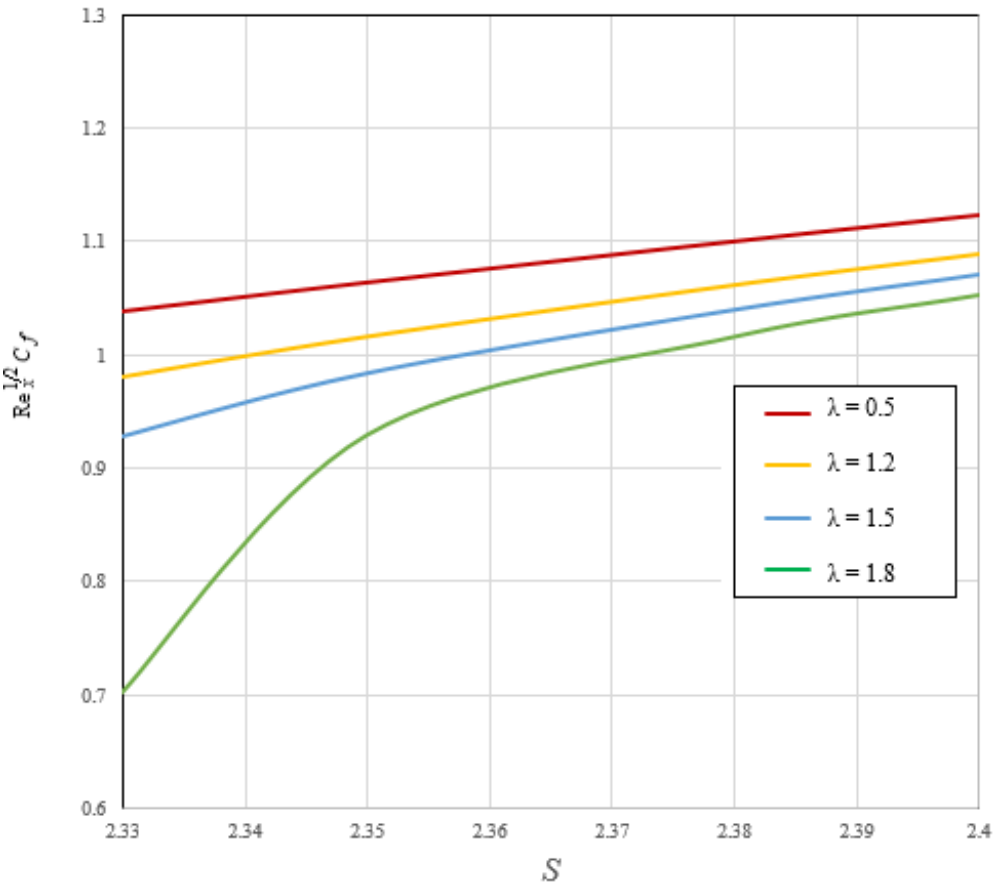

Fig. 2. $\mathrm{Re}_x^{1/2} C_f$ vs S for various values of λ where ε = -1, γ = 0.1, Pr = 10 and Z = -0.5

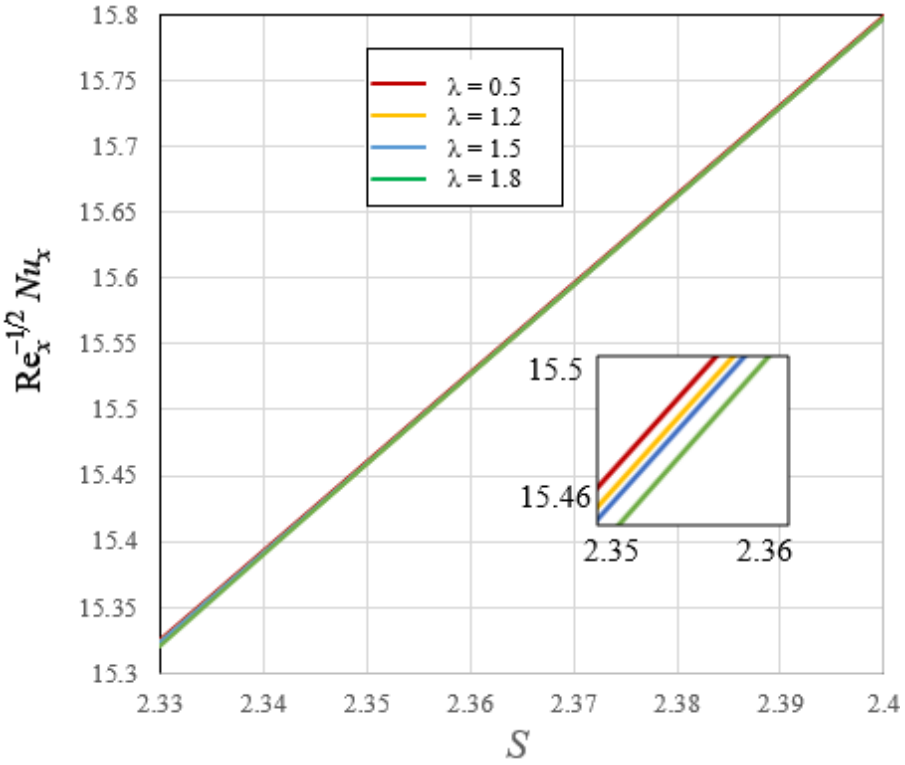

Fig. 3. $\mathrm{Re}_x^{-1/2} Nu_x$ vs *S* for various values of *λ* where *ε* = -1, *γ* = 0.1, Pr = 10 and *Z* = -0.5

Figure 4 and 5 illustrate how *λ* and *γ* affect variations in $\mathrm{Re}_x^{1/2} C_f$ and $\mathrm{Re}_x^{-1/2} Nu_x$ when *ε* = 1, Pr = 10 and *S* = *Z* = 0. For this model to be a non-Newtonian Reiner-Philippoff fluid model, ϕ_1 and ϕ_2 are both set to zero. The increase in $\mathrm{Re}_x^{-1/2} Nu_x$ and the decrease in $\mathrm{Re}_x^{1/2} C_f$ were both influenced by the rise in *λ*. When *γ* = 0.3, 0.5, 2 and *λ* = 1 (Newtonian fluid), the values of $\mathrm{Re}_x^{1/2} C_f$ = -0.67764793 and $\mathrm{Re}_x^{-1/2} Nu_x = 1.117224634$ remain unchanged (Table 8). Further, as *γ* increases, it becomes clear that the quantity of $\mathrm{Re}_x^{1/2} C_f$ rises when *λ* < 1 (dilatant fluid) and decreases when *λ* > 1 (pseudoplastic fluid), while the thermal rate yields opposite outcomes. Additionally, for future reference, Table 8 tabulates the computed values of $\mathrm{Re}_x^{1/2} C_f$ and $\mathrm{Re}_x^{-1/2} Nu_x$ with various values of *λ* and *γ*.

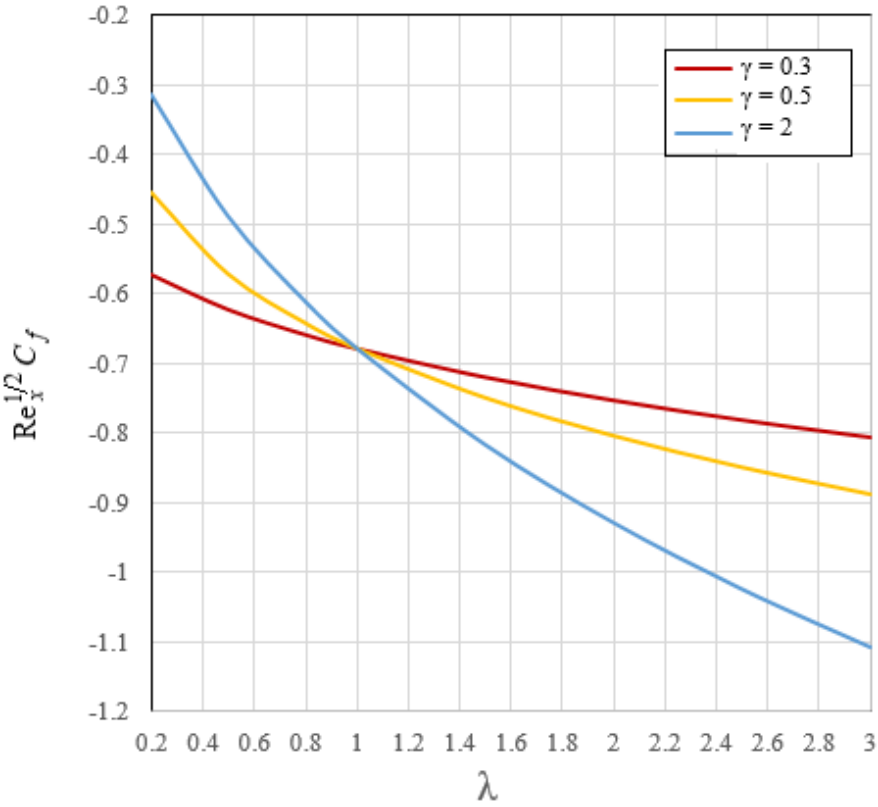

Fig. 4. $\mathrm{Re}_x^{1/2} C_f$ vs λ for various values of γ where $\varepsilon = 1$, Pr = 10 and $S = Z = 0$

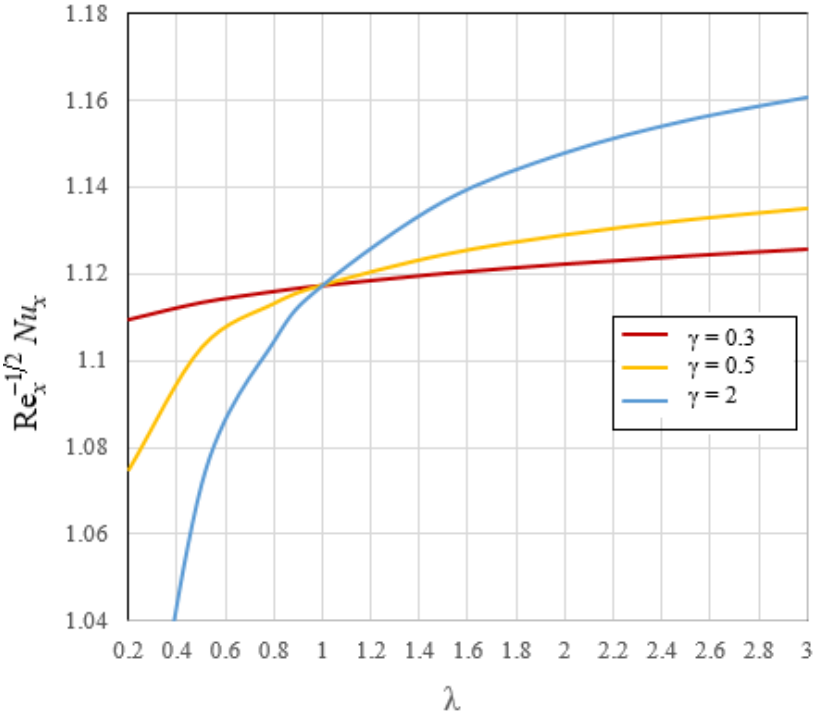

Fig. 5. $\mathrm{Re}_x^{-1/2} Nu_x$ vs λ for various values of γ where $\varepsilon = 1$, Pr = 10 and $S = Z = 0$

Table 8

Values of $\mathrm{Re}_x^{1/2} C_f$ and $\mathrm{Re}_x^{-1/2} Nu_x$ for λ and γ when ε = 1, Pr = 10 and $S = Z = \phi_1 = \phi_2 = 0$

λ	γ = 0.3		γ = 0.5		γ = 2	
	$\mathrm{Re}_x^{1/2} C_f$	$\mathrm{Re}_x^{-1/2} Nu_x$	$\mathrm{Re}_x^{1/2} C_f$	$\mathrm{Re}_x^{-1/2} Nu_x$	$\mathrm{Re}_x^{1/2} C_f$	$\mathrm{Re}_x^{-1/2} Nu_x$
0.2	-0.571405913	1.109494135	-0.454413417	1.074919188	-0.312096465	0.976476966
0.5	-0.621589532	1.113354604	-0.571307799	1.102878900	-0.487759442	1.071410812
0.8	-0.657721255	1.115877294	-0.641511772	1.113010824	-0.610294917	1.104426708
1.0	-0.677647983	1.117224634	-0.677647983	1.117224634	-0.677647983	1.117224634
1.5	-0.718769953	1.119945712	-0.748419875	1.124193035	-0.816690687	1.136574988
2.0	-0.752029995	1.122104847	-0.802981734	1.128741894	-0.929233695	1.147725714
2.5	-0.780309880	1.123916366	-0.848005566	1.132107848	-1.024871047	1.155141945
3.0	-0.805104451	1.125486397	-0.886660341	1.134776439	-1.108575709	1.160506653

This study also looks at the impact of volumetric concentration on a related topic. According to Table 9, it was shown that the $\mathrm{Re}_x^{1/2} C_f$ and $\mathrm{Re}_x^{-1/2} Nu_x$ improve higher when the concentration of Cu (ϕ_2) nanoparticles increases, while for Z = -1, the reverse behaviour is seen. A higher concentration of Cu nanoparticles produces more kinematic energy, which boosts the fluid particles' ability to transfer heat (Figure 6 and Figure 7). Additionally, it is seen that as Z and ϕ_2 increases, so do the values of $\mathrm{Re}_x^{-1/2} Nu_x$. This finding demonstrates that the synergistic effects mentioned by Sarkar *et al.,* [34] can increase the heat transfer rate when hybrid nanoparticles are added.

Figure 8 to 13 show several samples of the velocity $f'(\eta)$ and temperature $\theta(\eta)$ profiles for particular parameters. The boundary condition is asymptotically satisfied by these profiles, confirming the accuracy of the numerical findings. Figure 8 and 9 show the analysis with Reiner-Philippoff parameters considered for the velocity and temperature profiles. The profiles demonstrate that the fluid's velocity decreases as λ increases. The temperature profiles, however, exhibit the opposite behaviour. The analysis of the velocity and temperature profiles with variations in S and Z was shown in Figure 10 to 13, respectively (with fixed values of ϕ_1 = 0.01 and ϕ_2 = 0.02). Figure 10 and Figure 12 show that the increasing behaviour is seen as S and Z increase. Nevertheless, the temperature profiles shown in Figure 11 and 13 exhibit conflicting behaviour.

Table 9

Values of $\mathrm{Re}_x^{1/2} C_f$ and $\mathrm{Re}_x^{-1/2} Nu_x$ for selected values of ϕ_1, ϕ_2 and *Z* when ε = -1, Pr = 10 and *S* = 2.4 where ϕ_1 = Al_2O_3 and ϕ_2 = Cu

Z	$\phi_1 = 1.5\%$		$\phi_1 = 1\%$		$\phi_1 = 0.5\%$	
	$\phi_2 = 0.5\%$		$\phi_2 = 1\%$		$\phi_2 = 1.5\%$	
	$\mathrm{Re}_x^{1/2} C_f$	$\mathrm{Re}_x^{-1/2} Nu_x$	$\mathrm{Re}_x^{1/2} C_f$	$\mathrm{Re}_x^{-1/2} Nu_x$	$\mathrm{Re}_x^{1/2} C_f$	$\mathrm{Re}_x^{-1/2} Nu_x$
-1	0.646807266	15.696747986	0.575950470	15.703827628	0.505812081	15.710987918
0	1.281574759	15.705673614	1.329781786	15.714050900	1.376873461	15.722440787
1	1.451175837	15.707110093	1.580218334	15.716154487	1.707536315	15.725196750

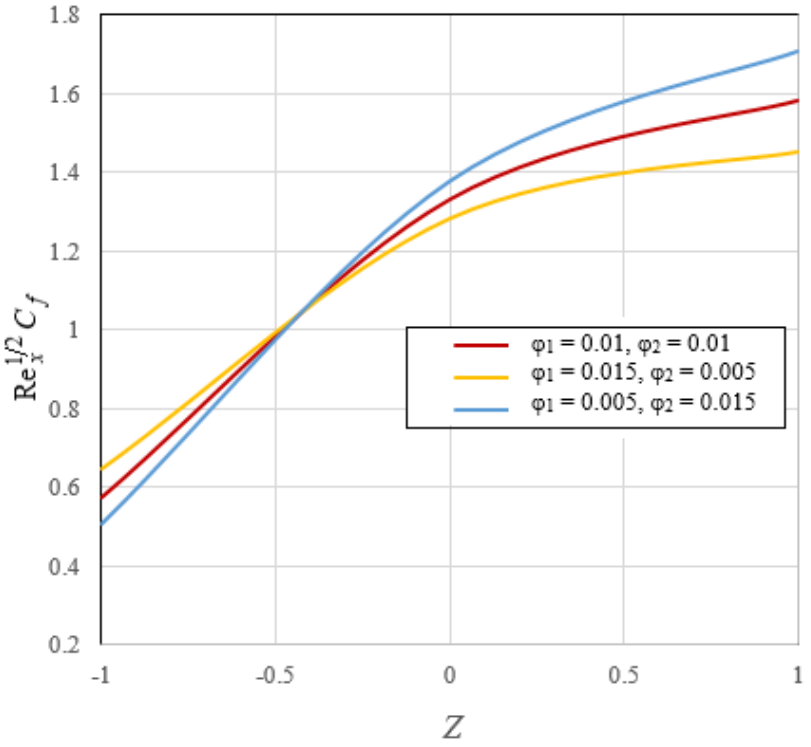

Fig. 6. $\mathrm{Re}_x^{1/2} C_f$ vs Z for various values of ϕ_1 and ϕ_2 where ε = -1, Pr = 10 and S = 2.4

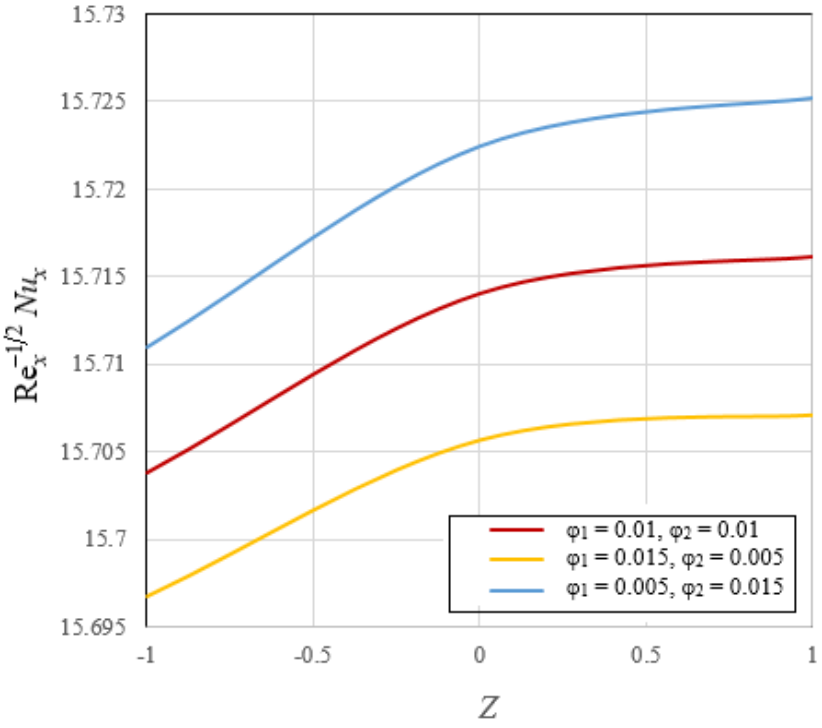

Fig. 7. $\mathrm{Re}_x^{-1/2} Nu_x$ vs Z for various values of ϕ_1 and ϕ_2 where ε = -1, Pr = 10 and S = 2.4

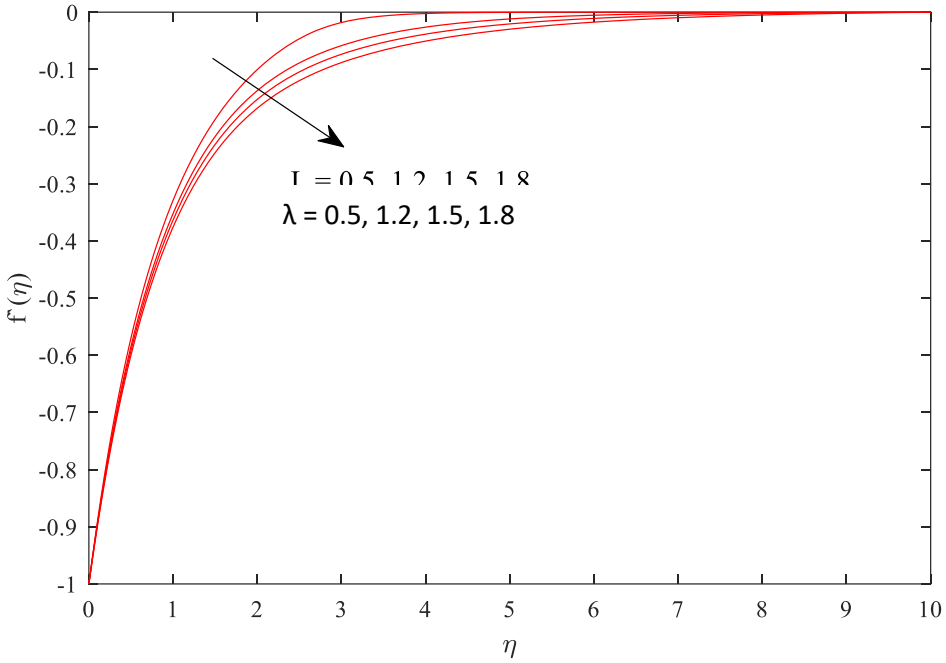

Fig. 8. Velocity profiles $f'(\eta)$ vs η for various values of λ where ε = -1, γ = 0.1, Pr = 10, S = 2.4 and Z = -0.5

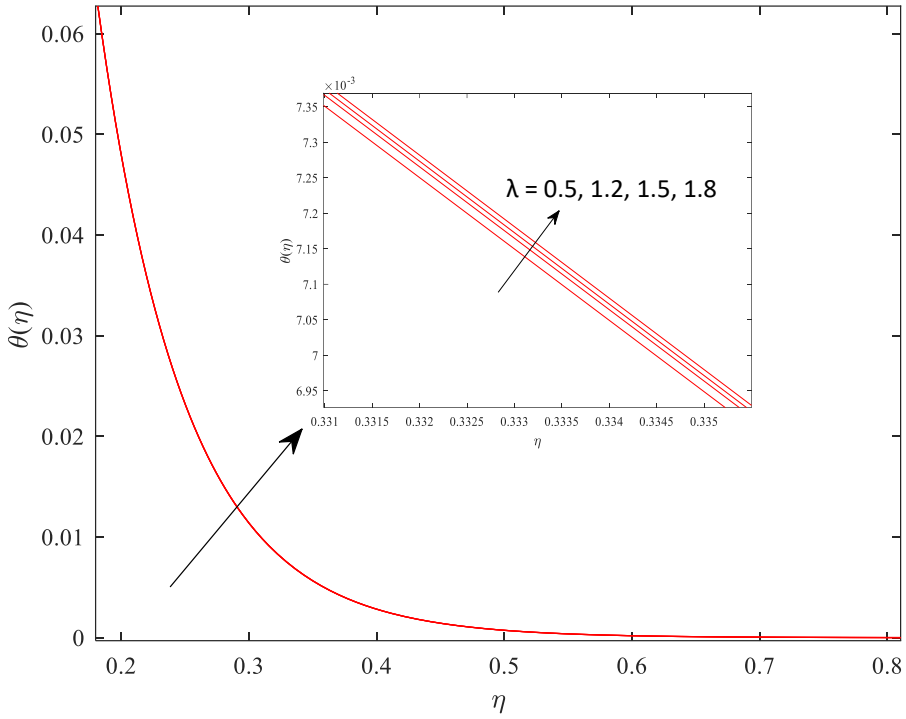

Fig. 9. Temperature profiles $\theta(\eta)$ vs η for various values of λ where ε = -1, γ = 0.1, Pr = 10, S = 2.4 and Z = -0.5

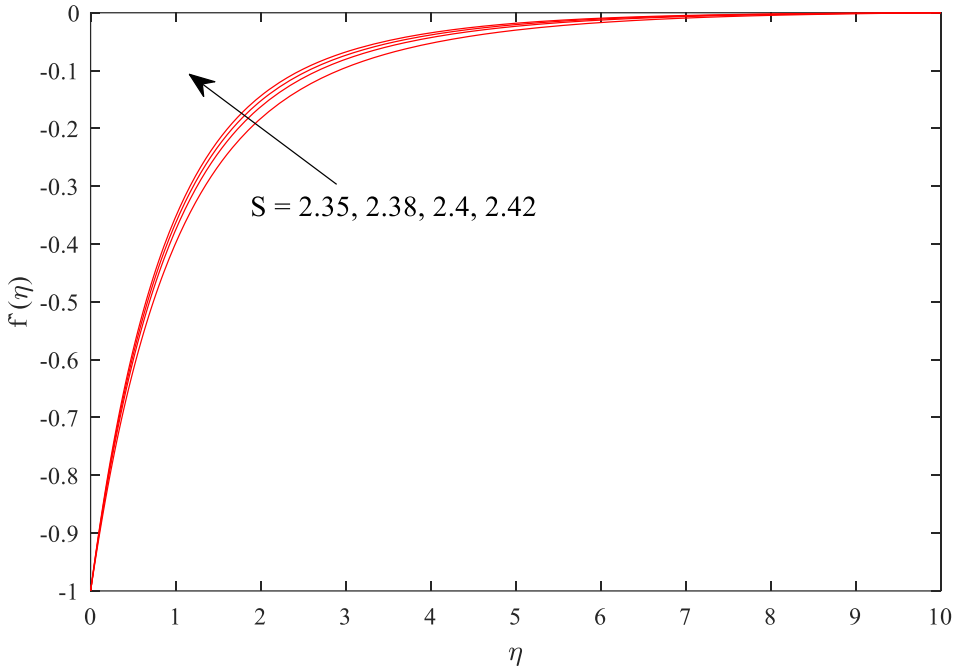

Fig. 10. Velocity profiles $f'(\eta)$ vs η for various values of S where ε = -1, λ = 1.5, γ = 0.1, Pr = 10 and Z = -0.5

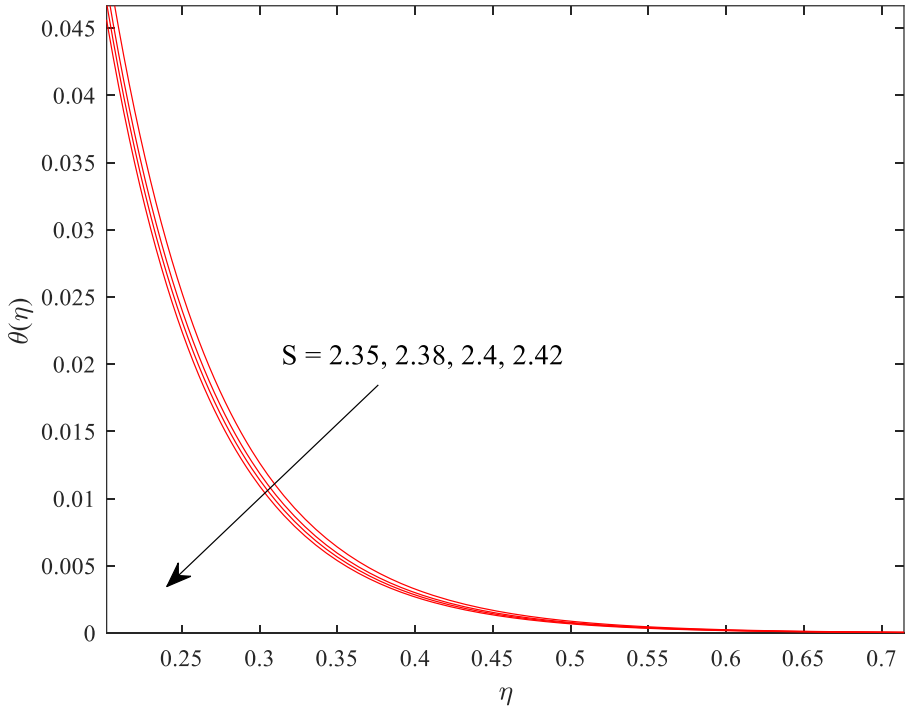

Fig. 11. Temperature profiles $\theta(\eta)$ vs η for various values of S where ε = -1, λ = 1.5, γ = 0.1, Pr = 10 and Z = -0.5

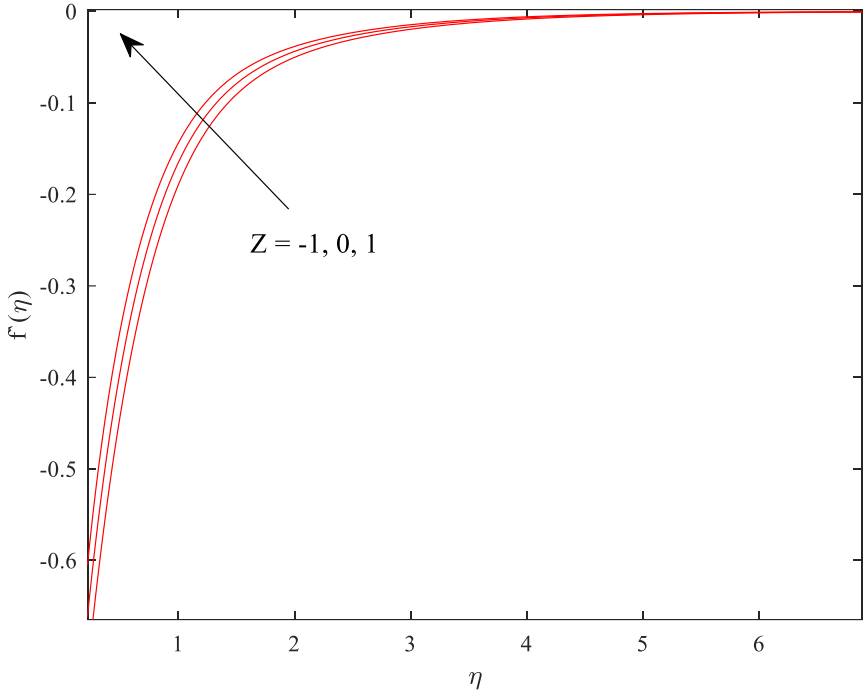

Fig. 12. Velocity profiles $f'(\eta)$ vs η for various values of Z where ε = -1, S = 2.4, λ = 1.5, γ = 0.1, Pr = 10, ϕ_1 = 0.01 and ϕ_2 = 0.02

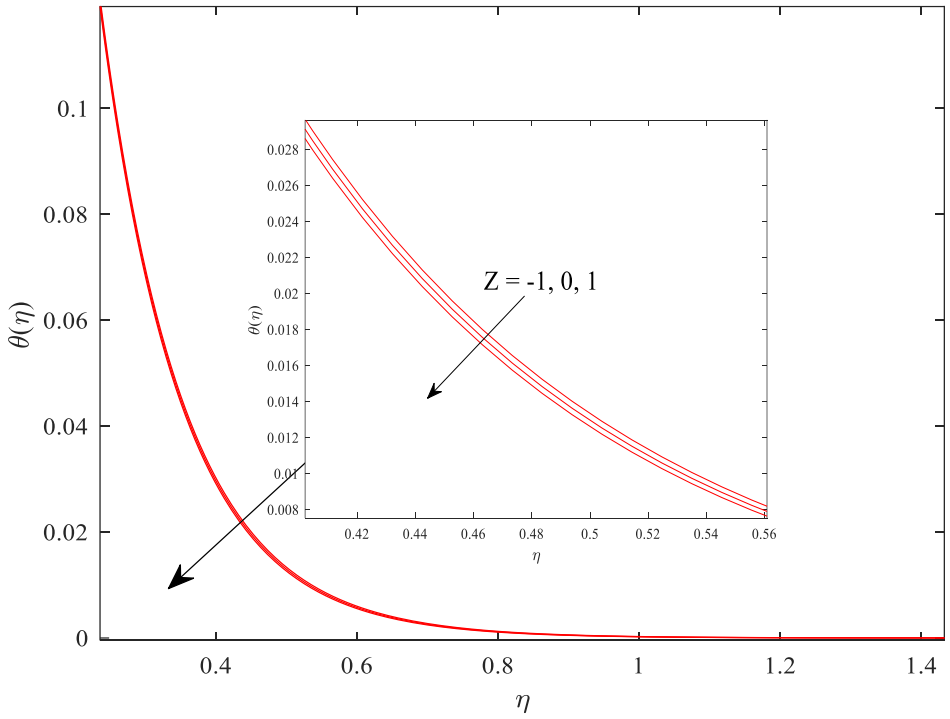

Fig. 13. Temperature profiles $\theta(\eta)$ vs η for various values of Z where ε = -1, S = 2.4, λ = 1.5, γ = 0.1, Pr = 10, ϕ_1 = 0.01 and ϕ_2 = 0.02

4. Conclusions

A mathematical analysis of mixed convection of the Reiner-Philippoff fluid flow past a shrinking sheet is established. The Reiner-Philippoff parameter shows that the increase in λ reduces the

velocity of the fluid while the reverse behaviour is attained for the temperature profiles. On the other hand, the increasing behaviour of the velocity profile is observed with the increasing of *S* and *Z* (where ϕ_1 = 0.01 and ϕ_2 = 0.02). Still, it shows a contradictory behaviour for the temperature profiles. The increase in the injection/suction parameter, mixed parameter and Prandtl number increase the local Nusselt number, while the increases in the Reiner-Philippoff parameter and Bingham number decrease the skin friction coefficient.

Acknowledgement
The authors want to acknowledge Universiti Malaysia Pahang for providing financial support under UIC221518. A deep appreciation also goes to Universiti Teknologi MARA (UiTM) Cawangan Johor, University of Kerbala, Universiti Teknikal Malaysia Melaka, Universiti Teknologi PETRONAS, Universitas Islam Riau and Telkom University for guidance and support.

References

[1] Krishnan, J. Murali, Abhijit P. Deshpande, and P. B. Sunil Kumar, eds. *Rheology of complex fluids*. New York: Springer, 2010. https://doi.org/10.1007/978-1-4419-6494-6
[2] Kapur, J. N., and R. C. Gupta. "Two dimensional flow of Reiner-Philippoff fluids in the inlet length of a straight channel." *Applied Scientific Research, Section A* 14 (1965): 13-24. https://doi.org/10.1007/BF00382227
[3] Cavatorta, Omar N., and Ruben D. Tonini. "Dimensionless velocity profiles and parameter maps for non-Newtonian fluids." *International Communications in Heat and Mass Transfer* 14, no. 4 (1987): 359-369. https://doi.org/10.1016/0735-1933(87)90057-1
[4] Hansen, A. G., and T. Y. Na. "Similarity solutions of laminar, incompressible boundary layer equations of non-Newtonian fluids." *Journal of Fluids Engineering* 90, no. 1 (1968): 71-74. https://doi.org/10.1115/1.3605067
[5] Na, Tsung-Yen. "Boundary layer flow of Reiner-Philippoff fluids." *International Journal of Non-Linear Mechanics* 29, no. 6 (1994): 871-877. https://doi.org/10.1016/0020-7462(94)90059-0
[6] Yam, K. S., S. D. Harris, D. B. Ingham, and I. Pop. "Boundary-layer flow of Reiner-Philippoff fluids past a stretching wedge." *International Journal of Non-Linear Mechanics* 44, no. 10 (2009): 1056-1062. https://doi.org/10.1016/j.ijnonlinmec.2009.08.006
[7] Ahmad, A., M. Qasim, and S. Ahmed. "Flow of Reiner-Philippoff fluid over a stretching sheet with variable thickness." *Journal of the Brazilian Society of Mechanical Sciences and Engineering* 39 (2017): 4469-4473. https://doi.org/10.1007/s40430-017-0840-7
[8] Gnaneswara Reddy, M., M. V. V. N. L. Sudharani, K. Ganesh Kumar, Ali J. Chamkha, and G. Lorenzini. "Physical aspects of Darcy-Forchheimer flow and dissipative heat transfer of Reiner-Philippoff fluid." *Journal of Thermal Analysis and Calorimetry* 141 (2020): 829-838. https://doi.org/10.1007/s10973-019-09072-0
[9] Kumar, K. Ganesh, M. Gnaneswara Reddy, M. V. V. N. L. Sudharani, S. A. Shehzad, and Ali J. Chamkha. "Cattaneo-Christov heat diffusion phenomenon in Reiner-Philippoff fluid through a transverse magnetic field." *Physica A: Statistical Mechanics and its Applications* 541 (2020): 123330. https://doi.org/10.1016/j.physa.2019.123330
[10] Sajid, T., M. Sagheer, and S. Hussain. "Impact of temperature-dependent heat source/sink and variable species diffusivity on radiative Reiner-Philippoff fluid." *Mathematical Problems in Engineering* 2020 (2020). https://doi.org/10.1155/2020/9701860
[11] Reddy, M. Gnaneswara, Sudha Rani, K. Ganesh Kumar, Asiful H. Seikh, Mohammad Rahimi-Gorji, and El-Sayed Mohmed Sherif. "Transverse magnetic flow over a Reiner-Philippoff nanofluid by considering solar radiation." *Modern Physics Letters B* 33, no. 36 (2019): 1950449. https://doi.org/10.1142/S0217984919504499
[12] Crane, Lawrence J. "Flow past a stretching plate." *Zeitschrift für angewandte Mathematik und Physik ZAMP* 21 (1970): 645-647. https://doi.org/10.1007/BF01587695
[13] Goldstein, Sydney. "On backward boundary layers and flow in converging passages." *Journal of Fluid Mechanics* 21, no. 1 (1965): 33-45. https://doi.org/10.1017/S0022112065000034
[14] Lund, Liaquat Ali, Zurni Omar, Sumera Dero, Dumitru Baleanu, and Ilyas Khan. "Rotating 3D flow of hybrid nanofluid on exponentially shrinking sheet: Symmetrical solution and duality." *Symmetry* 12, no. 10 (2020): 1637. https://doi.org/10.3390/sym12101637
[15] Zainal, Nurul Amira, Roslinda Nazar, Kohilavani Naganthran, and Ioan Pop. "Stability analysis of MHD hybrid nanofluid flow over a stretching/shrinking sheet with quadratic velocity." *Alexandria Engineering Journal* 60, no. 1 (2021): 915-926. https://doi.org/10.1016/j.aej.2020.10.020

[16] Khashi'ie, Najiyah Safwa, Norihan Md Arifin, Natalia C. Rosca, Alin V. Rosca, and Ioan Pop. "Three-dimensional flow of radiative hybrid nanofluid past a permeable stretching/shrinking sheet with homogeneous-heterogeneous reaction." *International Journal of Numerical Methods for Heat & Fluid Flow* 32, no. 2 (2022): 568-588. https://doi.org/10.1108/HFF-01-2021-0017

[17] Jamaludin, Anuar, Kohilavani Naganthran, Roslinda Nazar, and Ioan Pop. "MHD mixed convection stagnation-point flow of Cu-Al_2O_3/water hybrid nanofluid over a permeable stretching/shrinking surface with heat source/sink." *European Journal of Mechanics-B/Fluids* 84 (2020): 71-80. https://doi.org/10.1016/j.euromechflu.2020.05.017

[18] Waini, Iskandar, Anuar Ishak, and Ioan Pop. "Hybrid nanofluid flow and heat transfer over a nonlinear permeable stretching/shrinking surface." *International Journal of Numerical Methods for Heat & Fluid Flow* 29, no. 9 (2019): 3110-3127. https://doi.org/10.1108/HFF-01-2019-0057

[19] Yashkun, Ubaidullah, Khairy Zaimi, Nor Ashikin Abu Bakar, Anuar Ishak, and Ioan Pop. "MHD hybrid nanofluid flow over a permeable stretching/shrinking sheet with thermal radiation effect." *International Journal of Numerical Methods for Heat & Fluid Flow* 31, no. 3 (2020): 1014-1031. https://doi.org/10.1108/HFF-02-2020-0083

[20] Wahid, Nur Syahirah, Norihan Md Arifin, Mustafa Turkyilmazoglu, Mohd Ezad Hafidz Hafidzuddin, and Nor Aliza Abd Rahmin. "MHD hybrid Cu-Al_2O_3/water nanofluid flow with thermal radiation and partial slip past a permeable stretching surface: analytical solution." *Journal of Nano Research* 64 (2020): 75-91. https://doi.org/10.4028/www.scientific.net/JNanoR.64.75

[21] Abu Bakar, Shahirah, Norihan Md Arifin, Najiyah Safwa Khashi'ie, and Norfifah Bachok. "Hybrid nanofluid flow over a permeable shrinking sheet embedded in a porous medium with radiation and slip impacts." *Mathematics* 9, no. 8 (2021): 878. https://doi.org/10.3390/math9080878

[22] Waini, I., A. Ishak, and I. Pop. "Magnetohydrodynamic flow past a shrinking vertical sheet in a dusty hybrid nanofluid with thermal radiation." *Applied Mathematics and Mechanics* (2022): 1-14. https://doi.org/10.1007/s10483-022-2807-8

[23] Zainal, N. A., R. Nazar, K. Naganthran, and I. Pop. "Impact of anisotropic slip on the stagnation-point flow past a stretching/shrinking surface of the Al_2O_3-Cu/H_2O hybrid nanofluid." *Applied Mathematics and Mechanics* 41 (2020): 1401-1416. https://doi.org/10.1007/s10483-020-2642-6

[24] Merkin, J. H. "On dual solutions occurring in mixed convection in a porous medium." *Journal of engineering Mathematics* 20, no. 2 (1986): 171-179. https://doi.org/10.1007/BF00042775

[25] Ingham, D. B. "Singular and non-unique solutions of the boundary-layer equations for the flow due to free convection near a continuously moving vertical plate." *Zeitschrift für angewandte Mathematik und Physik ZAMP* 37 (1986): 559-572. https://doi.org/10.1007/BF00945430

[26] Ramachandran, N., T. S. Chen, and Bassem F. Armaly. "Mixed convection in stagnation flows adjacent to vertical surfaces." *ASME Journal of Heat and Mass Transfer* 110, no. 2 (1988): 373-377. https://doi.org/10.1115/1.3250494

[27] Zokri, Syazwani Mohd, Nur Syamilah Arifin, Muhammad Khairul Anuar Mohamed, Abdul Rahman Mohd Kasim, Nurul Farahain Mohammad, and Mohd Zuki Salleh. "Mathematical model of mixed convection boundary layer flow over a horizontal circular cylinder filled in a Jeffrey fluid with viscous dissipation effect." *Sains Malaysiana* 47, no. 7 (2018): 1607-1615. https://doi.org/10.17576/jsm-2018-4707-32

[28] Mahat, Rahimah, Noraihan Afiqah Rawi, Abdul Rahman Mohd Kasim, and Sharidan Shafie. "Heat generation effect on mixed convection flow of viscoelastic nanofluid: Convective boundary condition solution." *Malaysian Journal of Fundamental and Applied Sciences* 16, no. 2 (2020): 166-172. https://doi.org/10.11113/mjfas.v16n2.1367

[29] Khashi'ie, Najiyah Safwa, Norihan Md Arifin, Roslinda Nazar, Ezad Hafidz Hafidzuddin, Nadihah Wahi, and Ioan Pop. "Mixed convective flow and heat transfer of a dual stratified micropolar fluid induced by a permeable stretching/shrinking sheet." *Entropy* 21, no. 12 (2019): 1162. https://doi.org/10.3390/e21121162

[30] Waini, Iskandar, Anuar Ishak, Teodor Groşan, and Ioan Pop. "Mixed convection of a hybrid nanofluid flow along a vertical surface embedded in a porous medium." *International Communications in Heat and Mass Transfer* 114 (2020): 104565. https://doi.org/10.1016/j.icheatmasstransfer.2020.104565

[31] Waini, Iskandar, Anuar Ishak, and Ioan Pop. "Mixed convection flow over an exponentially stretching/shrinking vertical surface in a hybrid nanofluid." *Alexandria Engineering Journal* 59, no. 3 (2020): 1881-1891. https://doi.org/10.1016/j.aej.2020.05.030

[32] Turcu, R., A. L. Darabont, A. Nan, N. Aldea, D. Macovei, D. Bica, L. Vekas et al. "New polypyrrole-multiwall carbon nanotubes hybrid materials." *Journal of Optoelectronics and Advanced Materials* 8, no. 2 (2006): 643-647.

[33] Jana, Soumen, Amin Salehi-Khojin, and Wei-Hong Zhong. "Enhancement of fluid thermal conductivity by the addition of single and hybrid nano-additives." *Thermochimica Acta* 462, no. 1-2 (2007): 45-55. https://doi.org/10.1016/j.tca.2007.06.009

[34] Sarkar, Jahar, Pradyumna Ghosh, and Arjumand Adil. "A review on hybrid nanofluids: recent research, development and applications." *Renewable and Sustainable Energy Reviews* 43 (2015): 164-177. https://doi.org/10.1016/j.rser.2014.11.023

[35] Esfe, Mohammad Hemmat, Ali Alirezaie, and Mousa Rejvani. "An applicable study on the thermal conductivity of SWCNT-MgO hybrid nanofluid and price-performance analysis for energy management." *Applied Thermal Engineering* 111 (2017): 1202-1210. https://doi.org/10.1016/j.applthermaleng.2016.09.091

[36] Suresh, S., K. P. Venkitaraj, P. Selvakumar, and M. Chandrasekar. "Synthesis of Al_2O_3-Cu/water hybrid nanofluids using two step method and its thermo physical properties." *Colloids and Surfaces A: Physicochemical and Engineering Aspects* 388, no. 1-3 (2011): 41-48. https://doi.org/10.1016/j.colsurfa.2011.08.005

[37] Suresh, Sivan, K. P. Venkitaraj, Ponnusamy Selvakumar, and Murugesan Chandrasekar. "Effect of Al_2O_3-Cu/water hybrid nanofluid in heat transfer." *Experimental Thermal and Fluid Science* 38 (2012): 54-60. https://doi.org/10.1016/j.expthermflusci.2011.11.007

[38] Singh, Sumit Kr, and Jahar Sarkar. "Energy, exergy and economic assessments of shell and tube condenser using hybrid nanofluid as coolant." *International Communications in Heat and Mass Transfer* 98 (2018): 41-48. https://doi.org/10.1016/j.icheatmasstransfer.2018.08.005

[39] Farhana, K., K. Kadirgama, M. M. Rahman, M. M. Noor, D. Ramasamy, M. Samykano, G. Najafi, Nor Azwadi Che Sidik, and F. Tarlochan. "Significance of alumina in nanofluid technology: an overview." *Journal of Thermal Analysis and Calorimetry* 138 (2019): 1107-1126. https://doi.org/10.1007/s10973-019-08305-6

[40] Devi, SP Anjali, and S. Suriya Uma Devi. "Numerical investigation of hydromagnetic hybrid Cu-Al_2O_3/water nanofluid flow over a permeable stretching sheet with suction." *International Journal of Nonlinear Sciences and Numerical Simulation* 17, no. 5 (2016): 249-257. https://doi.org/10.1515/ijnsns-2016-0037

[41] Waini, Iskandar, Anuar Ishak, and Ioan Pop. "Unsteady flow and heat transfer past a stretching/shrinking sheet in a hybrid nanofluid." *International Journal of Heat and Mass Transfer* 136 (2019): 288-297. https://doi.org/10.1016/j.ijheatmasstransfer.2019.02.101

[42] Ahmad, Adeel. "Flow of ReinerPhilippoff based nano-fluid past a stretching sheet." *Journal of Molecular Liquids* 219 (2016): 643-646. https://doi.org/10.1016/j.molliq.2016.03.068

[43] Oztop, Hakan F., and Eiyad Abu-Nada. "Numerical study of natural convection in partially heated rectangular enclosures filled with nanofluids." *International Journal of Heat and Fluid Flow* 29, no. 5 (2008): 1326-1336. https://doi.org/10.1016/j.ijheatfluidflow.2008.04.009

[44] Takabi, Behrouz, and Saeed Salehi. "Augmentation of the heat transfer performance of a sinusoidal corrugated enclosure by employing hybrid nanofluid." *Advances in Mechanical Engineering* 6 (2014): 147059. https://doi.org/10.1155/2014/147059

[45] Khan, Ansab Azam, Khairy Zaimi, Suliadi Firdaus Sufahani, and Mohammad Ferdows. "MHD Mixed Convection Flow and Heat Transfer of a Dual Stratified Micropolar Fluid Over a Vertical Stretching/Shrinking Sheet With Suction, Chemical Reaction and Heat Source." *CFD Letters* 12, no. 11 (2020): 106-120. https://doi.org/10.37934/cfdl.12.11.106120

[46] Bakar, Fairul Naim Abu, and Siti Khuzaimah Soid. "MHD stagnation-point flow and heat transfer over an exponentially stretching/shrinking vertical sheet in a micropolar fluid with a Buoyancy effect." *Journal of Advanced Research in Numerical Heat Transfer* 8, no. 1 (2022): 50-55.

[47] Mohammed, H. A., O. A. Alawi, and N. A. Che Sidik. "Mixed convective nanofluids flow in a channel having forward-facing step with baffle." *Journal of Advanced Research in Applied Mechanics* 24, no. 1 (2016): 1-21.

[48] Bakar, Shahirah Abu, Norihan Md Arifin, and Ioan Pop. "Mixed Convection Hybrid Nanofluid Flow past a Stagnation-Point Region with Variable Viscosity and Second-Order Slip." *Journal of Advanced Research in Micro and Nano Engineering* 12, no. 1 (2023): 1-21. https://doi.org/10.37934/armne.12.1.121

[49] Khan, Ansab Azam, Khairy Zaimi, Suliadi Firdaus Sufahani, and Mohammad Ferdows. "MHD flow and heat transfer of double stratified micropolar fluid over a vertical permeable shrinking/stretching sheet with chemical reaction and heat source." *Journal of Advanced Research in Applied Sciences and Engineering Technology* 21, no. 1 (2020): 1-14. https://doi.org/10.37934/araset.21.1.114

[50] Cortell, Rafael. "Heat and fluid flow due to non-linearly stretching surfaces." *Applied Mathematics and Computation* 217, no. 19 (2011): 7564-7572. https://doi.org/10.1016/j.amc.2011.02.029

[51] Ferdows, M., Md Jashim Uddin, and A. A. Afify. "Scaling group transformation for MHD boundary layer free convective heat and mass transfer flow past a convectively heated nonlinear radiating stretching sheet." *International Journal of Heat and Mass Transfer* 56, no. 1-2 (2013): 181-187. https://doi.org/10.1016/j.ijheatmasstransfer.2012.09.020

[52] Waini, Iskandar, Abdul Rahman Mohd Kasim, Najiyah Safwa Khashi'ie, Nurul Amira Zainal, Anuar Ishak, and Ioan Pop. "Insight into Stability Analysis on Modified Magnetic Field of Radiative Non-Newtonian Reiner-Philippoff Fluid Model." *Journal of Applied and Computational Mechanics* 8, no. 2 (2022): 745-753.